

Simulating injection moulding of microfeatured components

T. Tofteberg^{1*} and E. Andreassen¹

¹SINTEF Materials and Chemistry, Oslo, Norway – terje.tofteberg@sintef.no; erik.andreassen@sintef.no

Numerical simulation of injection moulding of a microfeatured component is reported in this paper. The simulation is divided in two; first a large scale simulation of the main geometry is performed and then a microscale simulation of the structural details using the pressure from the large scale simulation as a boundary condition. The simulations show that even though the polymer solidifies in less than 5 ms, there is enough time to make a good replication of the microfeatures as has also been shown experimentally. It is also possible to isolate different physical effects influencing the replication. The shear heating in the microfeature is in this case not important. However, the shear thinning within the microfeatures helps replication significantly. The shear stress at the wall is in the lower range of where wall slip has been reported to occur for other polymer melts. Even though wall adhesion is not considered in these simulations, it is shown that the adhesion energy is comparable in size with the pressure-volume work required to push the polymer into the microfeature and could therefore be an important factor influencing replication.

Introduction

Microfeatured components are commonly used as optical storage media (CD, DVD Blu-ray Disc), and they are meeting new challenges in the world of microfluidics [1]. When patterning a polymer surface on the microscale the physical properties can be changed dramatically, e.g. to make superhydrophobic surfaces [2].

The simulations performed in this work relates to an experimental study in which a diffractive optical element (DOE) was injection moulded [3]. This DOE is an essential part of a low-cost infrared spectrometer, which e.g. can be used to identify different types of polymers. In Figure 1 the shape of the DOE is shown on the macro and microscale. The grating shown in part b) of the figure spans an area of 10 mm x 10 mm which means ~3000 periods. One of the materials used in the experiments was Topas 5013S-04, a Cyclic Olefin Copolymer (COC), and the simulations presented here will consider this material.

Previous attempts on simulating microfeatures

The specific problem related to the simulation of microfeatured parts is the large size scale ratios between the overall geometry and the microfeatures. In our case the height of the grating is less than 0.1 % of the thickness of the part that we are moulding. Trying to simulate both size scales in one simulation can lead to unphysical results [4, 5]. Another approach which is similar to the one employed in this work, is to first perform a large scale simulation considering only the overall geometry. Then the pressure and temperature field from this simulation is used as a boundary condition for a local simulation of the microfeature [6-8].

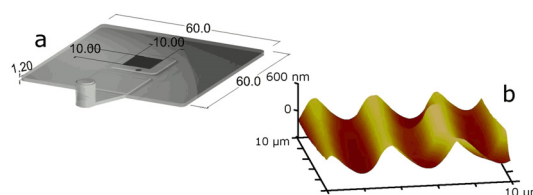


Figure 1 a) Drawing of the injection moulded part with dimensions [mm]. The microfeatures are located in the central square area and a pressure sensor located in the cavity opposite to the microfeatures is indicated with a dark grey circle. b) The topography of the microfeatures measured on an injection moulded DOE using AFM.

Experimental

The simulations were performed with ANSYS CFX 11.0 [9] and Moldflow MPI 6.1 [10]. CFX is a finite volume program developed as a general fluid mechanics solver while Moldflow is the most widely used injection moulding software. We have used Moldflow simulations for simulating the filling of the main geometry and used data from these simulations as boundary conditions for local simulations around the microfeatures.

Since Moldflow simulations are routinely done in both industry and academia we will not go into the computational details involved, but rather consider the novel microscale simulation. On the microscale we have been solving a multiphase problem where we have considered both the flow of air and of a polymer melt within a Ni mould. The effect of the mould is only taken into account as a boundary condition. The multiphase problem is solved by using the so called inhomogeneous model in CFX, meaning that the two phases have two separate flow fields. These fields are calculated by solving two sets of Navier-Stokes equations. The two flow fields are independent except for in the interphase region where they interact via interphase transfer terms.

Governing equations

The equation of continuity is written for each phase as

$$\frac{\partial(\alpha_i \rho_i)}{\partial t} + \mathbf{u}_i \cdot \nabla(\alpha_i \rho_i) = 0, \quad (1)$$

where \mathbf{u} is the velocity vector, t the time, ∇ the divergence operator, α the volume fraction and ρ the density. The subscript i describes the phase and can be either polymer melt or air. The melt is treated as a generalized Newtonian fluid and the momentum balance is written

$$\frac{\partial(\alpha_i \rho_i \mathbf{u}_i)}{\partial t} + \mathbf{u}_i \cdot (\nabla(\alpha_i \rho_i \mathbf{u}_i)) = -\alpha_i \nabla p + \nabla \cdot (\alpha_i \eta_i (\nabla \mathbf{u}_i + (\nabla \mathbf{u}_i)^T)) + \mathbf{M}_{ij} \quad (2)$$

where p is the pressure and η the viscosity. \mathbf{M}_{ij} is the interphase transfer term which obeys Newton's third law by having $\mathbf{M}_{ij} = -\mathbf{M}_{ji}$ and is expressed as

$$\mathbf{M}_{ij} = C_D \rho \alpha_i \alpha_j |\mathbf{u}_i - \mathbf{u}_j| (\mathbf{u}_j - \mathbf{u}_i), \quad (3)$$

where C_D is a constant interphase transfer coefficient. As can be seen, if α_i is either zero or unity the transfer term vanishes. The density ρ is the total density taken as a linear interpolation between the two phases, i.e. $\rho = \alpha_i \rho_i + \alpha_j \rho_j$

There are now 9 unknowns, the two volume fractions, the six velocity components and the pressure. The equations required are two times Equation (1) (one for each phase), six times Equation (2) (two phases, three components), and the fact that the volume fractions add to unity. In addition we will introduce a new variable, the temperature.

The temperature field is shared by both fluids and in the energy equation we include conductive and convective heat transfer and a term describing viscous dissipation.

$$\left(\frac{\partial(\rho c_p T)}{\partial t} + \mathbf{u} \cdot (\nabla \rho c_p T) \right) = \nabla \cdot (\kappa \nabla T) + \eta \dot{\gamma}^2 \quad (4)$$

T is the temperature, c_p is the heat capacity, κ is the heat conductivity and $\dot{\gamma}$ is the shear rate. All variables and parameters, including the velocity field in Equation (4) are taken as a linear interpolation using the same procedure as described for the density in Equation (3).

Computational domain and mesh

The computational domain for the microscale simulation is shown in Figure 2. It represents one period of the diffractive grating, 600 nm high and 3 μ m long. By using periodic boundary conditions the

simulation is actually of an infinite series of such peaks. It has previously been shown that placing the inlet directly at the microfeature (where the interphase is located in Figure 2) neglects important contributions to the pressure loss and temperature field [4]. Because of this we also include the lower part of the geometry. The unstructured mesh is seen in the same figure.

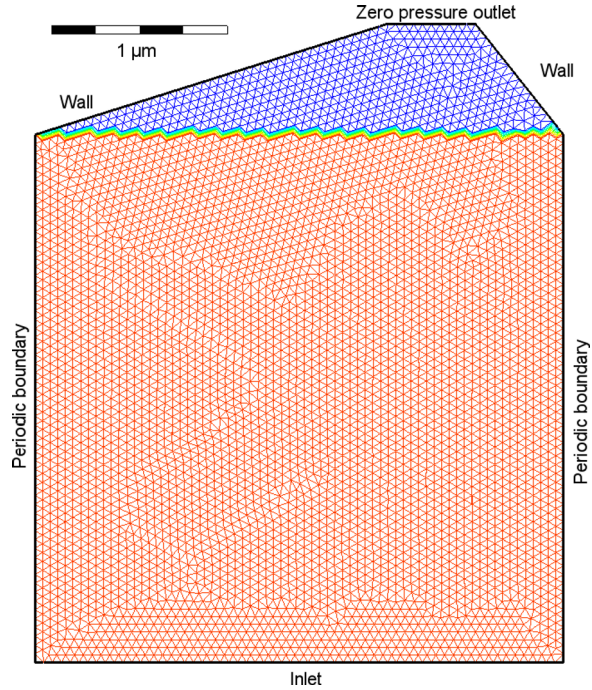


Figure 2 The computational domain for the microscale simulation representing one period of the diffractive grating shown in Figure 1b. The mesh is uniform and unstructured. The initial state of the volume fraction variable is shown with red indicating polymer and blue air.

Boundary conditions

At the walls we have applied no-slip conditions for the polymer and free slip for the air. A heat transfer coefficient is defined to be $h = 5000 \text{ W/m}^2 \text{ K}$ at the wall.

At the top of the computational domain we have a zero pressure outlet where air is allowed to escape from the simulation.

There are two periodic boundaries, meaning that any fluid leaving on the right side will reappear on the left, thus mimicking that there is a repeating grating consisting of an infinite number of copies of the geometry in Figure 2.

An the inlet we prescribe a time dependent pressure obtained from Moldflow simulations of the entire geometry shown in Figure 1a. In the experimental work described in ref. [3] the cavity pressure was measured and as can be seen in Figure 3, there is very good

agreement between simulated and measured cavity pressure.

The temperature of the melt entering through the inlet is set so that the temperature gradient is constant.

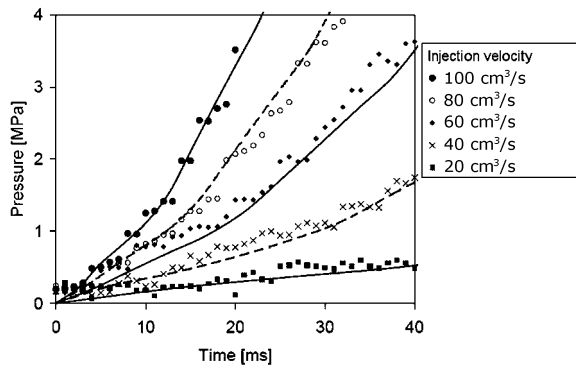


Figure 3 Measured (symbols) and simulated (lines) cavity pressure vs. time. Mould temperature 110 °C. The location of the pressure sensor is indicated in Figure 1a.

Initial conditions

The microscopic simulation starts as the flow front hits the microfeature. Since the microfeature is so small compared to the thickness of the part, the flow front is essentially parallel with the mould wall it hits and the initial shape of the flow front used in the simulations can be seen in Figure 2. The initial temperature is set to be the same as the melt temperature in nozzle of the injection moulding machine. This initial temperature is based on Moldflow simulations of the flow front temperature as can be seen in Figure 4, where it can be seen that the temperature of the flow front is almost uniform in space.

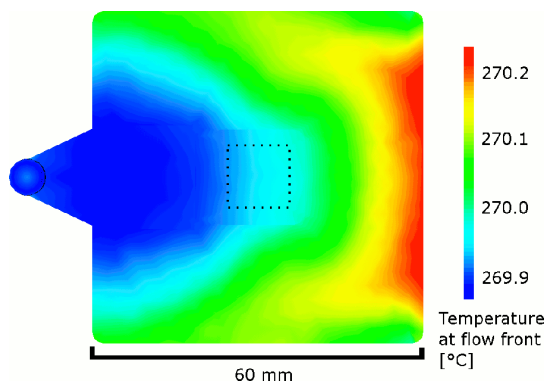


Figure 4 The simulated temperature at the flow front for an injection molded DOE with injection velocity 20 cm³/s, mould temperature 60°C and inlet melt temperature 270°C. The microfeathered area is shown with a dotted line.

Material properties

The viscosity of the polymer is described using a six parameter Cross-WLF model which is the same model used in the Moldflow simulations.

$$\eta(T, \dot{\gamma}) = \frac{\eta_o(T)}{1 + \left(\frac{\eta_o(T) \dot{\gamma}}{\tau^*} \right)^{1-n}} \quad (5)$$

$$\eta_o(T) = D1 \exp \left\{ \frac{-A1(T - D2)}{A2 + (T - D2)} \right\}$$

The parameters used in this equation were taken from the Moldflow database. All physical properties for both fluids, except for the melt viscosity are set to a constant value. Values are given in Table 1. In order to improve convergence, the viscosity of air was increased. It is however still so low that the flow of the air does not influence the flow of the polymer.

Table 1 Physical constants for the materials used in the simulations. The six first parameters are Cross-WLF parameters for equation (5).

		COC	Air
<i>A1</i>	[-]	37.16	0
<i>A2</i>	[K]	51.6	0
<i>D1</i>	[Pa·s]	4.884·10 ¹⁵	0.1
<i>D2</i>	[Pa·s]	343.15	0
τ^*	[Pa]	3433	0
<i>n</i>	[-]	0.4617	0
ρ	[kg/m ³]	1049.3	1
κ	[W/mK]	0.163	0.026
<i>c_p</i>	[J/kgK]	1800	1004

2D/3D simulation

Using CFX, all simulations are performed in 3D. In this case we only need a 2D simulation. This is done by making a mesh which is one element thick in the out of plane direction. Symmetry boundary conditions are applied on the two faces parallel to the computational domain.

Results and Discussion

Figure 5 shows the flow front as a function of time and processing parameters. It can be seen that the speed of the flow front gradually decreases before coming to a stop because the melt has been cooled by the mould wall. When increasing the injection velocity (going from left to right in the figure) the degree of filling increases, as when increasing the mould temperature (going from top to bottom in the figure). It was also found experimentally that the degree of replication changed from ~20% at the settings in the upper left corner to ~100% at the settings in the lower right corner. [3]

The results presented next all relate to the simulation marked T110 v100 in Figure 5 (middle-right), which is one of the simulations with the highest injection velocity and where we expect to have the highest shear rates.

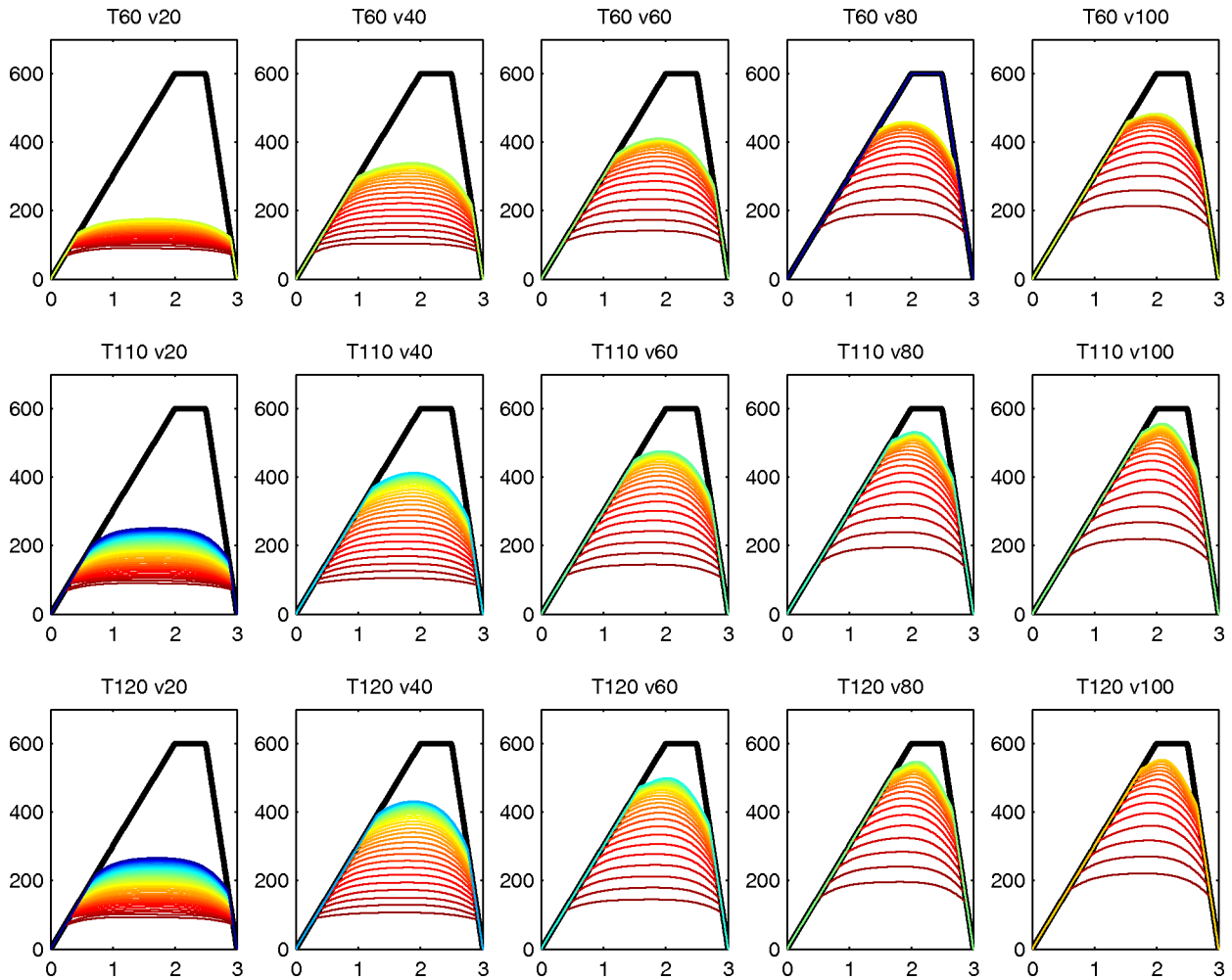


Figure 5 The simulated flow front as a function of time and processing settings. The thick black line is the mould wall and the contours are the flow front separated by 0.1 ms. T refers to the mould temperature [°C] and v to the injection velocity [cm³/s]. The x-axis is the horizontal distance [μm] and the y-axis the vertical [nm]. For all simulations the flow front was horizontal y=0 at t=0 and the lower contour represents the flow front at t = 0.6 ms. Contours with the same colour indicate the same time value.

Temperature distribution

The rate of cooling for the polymer melt as it hits the mould can be seen in Figure 6. It can be seen here that the melt is cooled very rapidly (2-3 ms) from the melt temperature of 270 °C and down to a temperature around 160 °C where the viscosity increases to such high levels that the polymer stops behaving like a liquid and the flow front stops as seen in Figure 5. When the viscosity rises above a certain level we are no longer capable of obtaining convergence and the simulation is aborted. It can also be seen in Figure 6, that the difference between the maximum and minimum temperature within the computational domain is small. This is because the microfeature (and the computational domain) is so small that any thermal gradient that may exist will immediately vanish due to thermal conduction.

Also note that the temperature first decreases relatively slowly before the rate increases and decreases again. This is because the heat flow is proportional to the temperature difference between the melt and the mould and to the contact area. At the start of the simulation the contact area is small leading to a relatively small cooling rate. Then the contact area increases and with it also the cooling rate before, near the end of the simulation, the temperature difference between the mould and the melt is getting smaller and the cooling rate decreases.

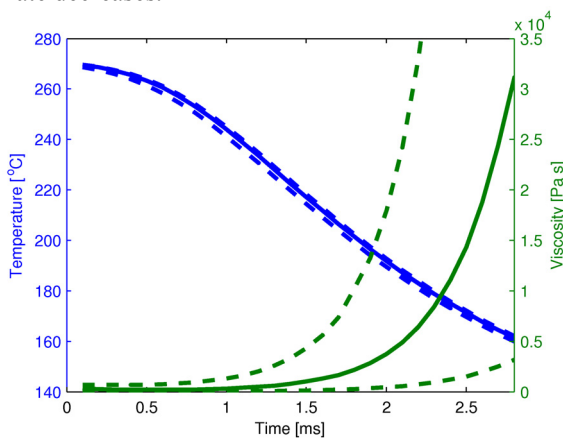


Figure 6 Simulated temperature and viscosity in the computational domain for an injection moulded DOE with settings: $T_{\text{mold}} = 110 \text{ }^\circ\text{C}$, $v_{\text{inj}} = 100 \text{ cm}^3/\text{s}$ and $h = 5000 \text{ W/m}^2\text{K}$. The solid lines show the average value and the dotted lines show the max and min value at each time step.

Shear rates

The polymer melt is highly shear thinning. Is shear thinning in the microfeature an important factor for the replication of microfeatures? The shear rates for the same part as is shown in Figure 6 (high injection speed) are shown in Figure 7. The highest shear rate is $\sim 2000 \text{ s}^{-1}$ at this time step. According to the Cross-WLF model used, this is enough to reduce the viscosity by more than a factor 10 relative to the zero shear rate

viscosity. Hence, the shear thinning effect seems to be important, also within the microfeatures.

It can also be noted that the maximum shear stress at the wall observed during the simulations was $\sim 0.1 \text{ MPa}$ which in the same order of magnitude as the values where wall slip has been reported to occur for linear polyethylene melts [11,12]. No data have been found discussing the critical shear stress for wall slip with COC melts.

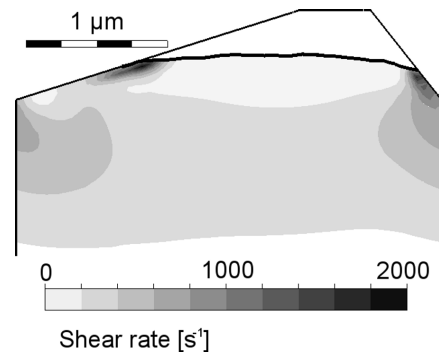


Figure 7 Simulated shear rates for the injection moulded part from Figure 6 at $t = 0.8 \text{ ms}$. It can be seen that the shear rates are well above 100 s^{-1} , approaching 2000 s^{-1} near the wall at the flow front.

Shear heating

It is of importance to know if the local shear heating in the microfeature is a determining factor influencing replication. The local rate of shear heating can be written as $\eta\dot{\gamma}^2$. If we integrate this variable in space, we obtain the total effect [W] of the shear heating within the computational domain. The results are shown in Figure 8 for the same simulation as in Figure 6. The total effect increases at the beginning of the simulation as the pressure increases, but when the polymer melt solidifies the shear rate drops and the shear heating falls with it. Integration in time gives the total energy produced by shear heating:

$$E_{\text{shear}} = \int_0^t \int_V \eta \dot{\gamma}^2 dV dt$$

The curve in Figure 8 was integrated up to 2.5 ms, and the total energy due to shear heating was found to be 43 kJ/m^3 . Dividing this energy by ρc_p gives an estimated temperature increase of $0.02 \text{ }^\circ\text{C}$. This shows that the shear heating within the microfeature in this case is of minute importance and could have been removed from Equation (4), without much influence on the results.

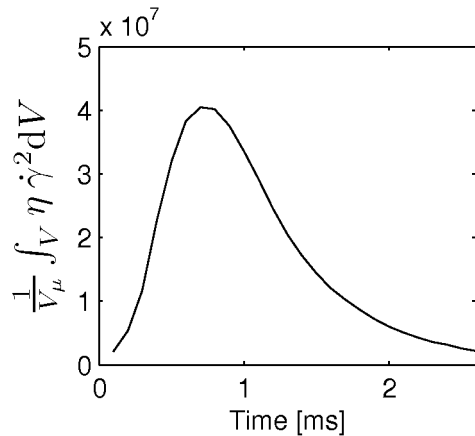


Figure 8 The simulated local shear rate integrated over the entire computational domain V , divided by the volume of the microfeature V_μ [W/m^3]. Same simulation settings as in Figure 6

Adhesion effects

The total work that forced the polymer melt into the microfeature is the same as the work dissipated as heat in the simulation. It has been argued that for submicrometer structures, where the surface area is large compared to the volume, the adhesion force between the wall and the melt may be an important factor influencing replication [13]. The ratio between the total energy required to force the polymer into the microfeature and the mould surface area of the microfeature is in this case $0.012 \text{ J}/\text{m}^2$.

It has been reported that the adhesion energy between a steel wall and polyethylene (PE) is $0.02 - 0.04 \text{ J}/\text{m}^2$ depending on the grade of PE. We would expect that the adhesion energy between the mould wall (Nickel in this case) and the polymer melt (a cyclic olefin copolymer) is of the same order of magnitude as this, but we do not have specific measurements relating to these two materials. It is still likely that the adhesion energy between the mould wall and the polymer plays an important role in the replication of micrometer sized features.

Simulation time

The simulations performed in this work took approximately 48 hours on one core of an Intel Core 2 Duo T7600 2.33GHz processor while the author had other things to do on the second core.

Conclusions

We have demonstrated a novel approach to simulate injection moulding of microfeatured components. With this method it is possible to get a reasonable estimate for the replication quality of microfeatures. The model correctly accounts for the positive correlation observed experimentally between injection speed and degree of replication and between mould temperature and degree of replication.

The simulations show that even though the temperature of the polymer melt decreases to below an effective no-flow temperature in 2-3 ms, there is still enough time to fill the micrometer sized structural details.

It is also possible to isolate physical phenomena influencing the replication quality. It is observed that the shear heating in the microfeatures in this case can be neglected, that the shear thinning is important for the filling of the microfeatures and that the flow regime is similar to regimes where wall slip has been observed to occur for polyethylene melts.

The simulations also indicate that the adhesion energy between the mould wall and the polymer is important when replicating micrometer sized or smaller features.

References

1. G. M. Whitesides *Nature* 2006, 442, 368.
2. E. Puukilainen; T. Rasilainen; M. Suvanto; T. A. Pakkanen *Langmuir* 2007, 23, 7263.
3. T. Tofteberg; H. Amédéo; E. Andreassen *Polym. Eng. Sci.* 2008, Submitted.
4. T. Tofteberg; E. Andreassen in PPS Europe/Africa Regional Meeting, Gothenburg, 2007.
5. L. Yu; L. J. Lee; K. W. Koelling *Polym. Eng. Sci.* 2004, 44, 1866.
6. D. Yao; B. Kim *J. Micromech. Microeng.* 2002, 12, 604.
7. S. W. Kim; L. S. Turng *Polym. Eng. Sci.* 2006, 46, 1263.
8. T. Eriksson; H. K. Rasmussen *J. Non-Newton. Fluid.* 2005, 127, 191.
9. ANSYS CFX-11.0, *ANSYS Europe Ltd.*, 2007.
10. Moldflow Plastics Insight (MPI) 6.1, *Moldflow Corporation*, 2007.
11. M. M. Denn *Annual Review of Fluid Mechanics* 2001, 33, 265.
12. S. H. Anastasiadis; S. G. Hatzikiriakos *Journal of Rheology* 1998, 42, 795.
13. H. Pranov; H. K. Rasmussen; N. B. Larsen; N. Gadegaard *Polym. Eng. Sci.* 2006, 46, 160.